

Phased arrays of buried-ridge InP/InGaAsP diode lasers

E. Kapon, L. T. Lu, Z. Rav-Noy, M. Yi,^{a)} S. Margalit, and A. Yariv
California Institute of Technology, Pasadena, California 91125

(Received 18 October 1984; accepted for publication 2 November 1984)

Phase-locked arrays of buried-ridge InP/InGaAsP lasers, emitting at $1.3\ \mu\text{m}$, were grown by liquid phase epitaxy. The arrays consist of index-guided, buried-ridge lasers which are coupled via their evanescent optical fields. This index-guided structure makes it possible to avoid the occurrence of lower gain in the interchannel regions. As a result, the buried-ridge arrays oscillate mainly in the fundamental supermode, which yields single lobed, narrow far-field patterns. Single lobed beams less than 4° in width were obtained from buried-ridge InP/InGaAsP phased arrays up to more than twice the threshold current.

Most phase-locked arrays of diode lasers demonstrated thus far were based on the GaAs/GaAlAs material system.¹⁻⁴ However, high power InP/InGaAsP phased arrays, emitting in the longer wavelength range ($1.1\text{--}1.6\ \mu\text{m}$), are also of interest, mainly for applications in long-haul optical communication systems. In particular, the output wavelength selectivity and tunability which is exhibited by properly designed phased arrays⁵⁻⁷ may be of importance in optical communication applications.

An array of gain-guided InP/InGaAsP lasers, in which the coupling between the lasers was assisted by diffraction sections, has been demonstrated by Chen *et al.*⁸ In the present letter we report on the fabrication and the performance of phased arrays of buried-ridge InP/InGaAsP lasers emitting at $1.3\ \mu\text{m}$. The individual lasers in these arrays are index guided, due to a "soft" effective index distribution which is introduced by the buried-ridge configuration. This soft index profile ensures effective coupling between nearest neighbor lasers via their evanescent optical fields. Since the channels in these arrays are defined by a built-in refractive index distribution, it is possible to have a uniform gain distribution across their elements while maintaining the channel definition. This is in contrast to gain-guided arrays, in which the interchannel regions are necessarily more lossy. Thus, one can avoid the domination of the highest order supermode, whose nodal points are located in these lossy, interchannel regions,⁹ which frequently occurs in (uniform) gain-guided arrays.¹ The InP/InGaAsP buried-ridge arrays exhibited mostly single lobed beams with small divergence which indicated oscillation mainly in the fundamental supermode.

The schematic cross section of the InP/InGaAsP buried-ridge array is shown in Fig. 1. The arrays were grown by two steps of liquid phase epitaxy (LPE). First, a double heterostructure consisting of $2.5\ \mu\text{m}$ $n\text{-InP}$ (Sn doped, $8 \times 10^{17}\ \text{cm}^{-3}$), $0.2\ \mu\text{m}$ InGaAsP ($\lambda_g = 1.3\ \mu\text{m}$, undoped), and $\sim 1\ \mu\text{m}$ $p\text{-InP}$ (Zn doped, $10^{18}\ \text{cm}^{-3}$) was grown on an $n^+\text{-InP}$ substrate. Eight parallel channels, each $\sim 3\ \mu\text{m}$ wide and on $5\text{-}\mu\text{m}$ centers, were then formed along the $[01\bar{1}]$ direction by etching with 10% iodic acid solution through a SiO_2 mask. The groove depth was $\sim 0.5\ \mu\text{m}$. Next, the SiO_2 was removed, and a $p\text{-InGaAsP}$ layer ($\lambda_g = 1.2\ \mu\text{m}$, Zn doped, $2 \times 10^{18}\ \text{cm}^{-3}$), $1\ \mu\text{m}$ thick, was grown on the grooved wafer. A stripe Cr/Au contact, $\sim 50\ \mu\text{m}$ wide, was fabricated above the array channels. Finally, the wafer was

lapped and AuGe/Au contact layer was evaporated on the n side.

The difference in the refractive index of the etched $p\text{-InP}$ material and that of the regrown $p\text{-InGaAsP}$ material gives rise to periodic variation in the effective index of the optical mode guided by the active layer (see Fig. 1). When this effective index variation is small enough, one can calculate the array supermodes by using the effective index method.¹⁰ In that case, the effective index beneath the etched grooves will be larger, since the refractive index of the InGaAsP material is larger than that of the InP material. This results in eight index-guided channels (see Fig. 1) which are strongly coupled due to the small effective index differences and the close channel proximity.

The buried-ridge arrays were tested under low duty cycle pulsed operation (200-ns pulses). Typical threshold currents of $250\text{-}\mu\text{m}$ -long devices were about 400 mA. The near-field and the far-field radiation patterns of the arrays were displayed on a monitor by using an infrared vidicon camera. The intensity distributions of the various patterns were then obtained by employing a video analyzer.

Most of the arrays that were tested exhibited single lobed far-field patterns directed perpendicular to the laser facet. A typical far-field intensity distribution, measured parallel to the junction plane, is shown in Fig. 2 for several values of the array current. The insert shows a photograph of the far-field pattern. Near threshold, the measured full width at half-maximum power (FWHP) was 2.7° . The calculated FWHP of the fundamental supermode pattern of a uniform, eight-element array with $5\text{-}\mu\text{m}$ period emitting at $\lambda = 1.3\ \mu\text{m}$, is 2° . The deviation of the calculated result from the measured one may be the result of differences in the channel parameters, brought about by small nonuniformities in the dimensions of the etched grooves. Such nonuniform channels may yield narrower near-field envelopes and,

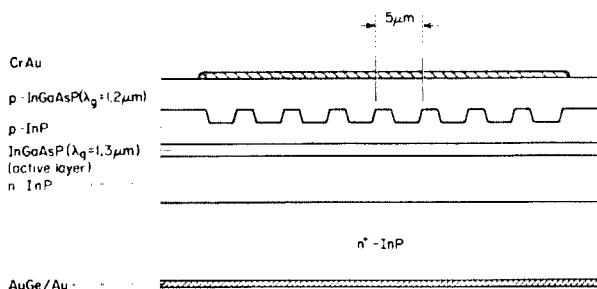


FIG. 1. Schematic cross section of the buried-ridge array.

^{a)} Visiting Associate from Jilin University, Changchun, China.

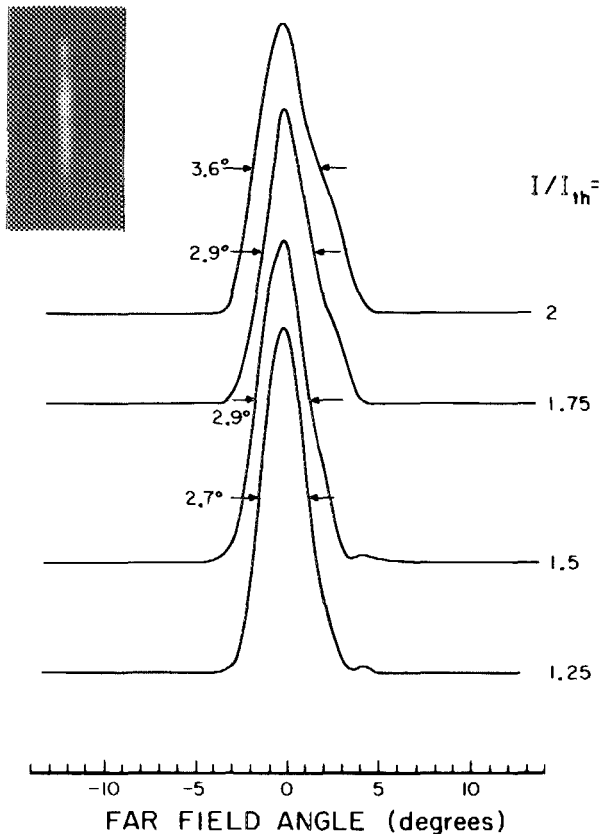


FIG. 2. Typical far-field pattern of the buried-ridge phased arrays, measured parallel to the junction plane at various array currents. The threshold current was $I_{th} = 400$ mA. The insert shows a photograph of the far field.

hence, broader far-field lobes, compared to those of uniform arrays.¹¹ At higher currents, the beam divergence increased and reached 3.6° at twice the threshold current. The additional structure in the far-field pattern suggests that this broadening is due to the excitation of higher order supermodes.⁹ For our phased arrays, the calculated far-field pattern of supermode $\nu = 2$ consists of two main lobes whose peaks are separated by 2.9° , with total FWHP of 4.4° , assuming a uniform array.⁹ It should be noted that the far-field patterns shown in Fig. 2 are narrower than those exhibited by the diffraction coupled InP/InGaAsP array⁸ and are less susceptible to the increase in the pump current. This indicates an efficient phase locking among the elements of the buried-ridge array as well as better discrimination against the higher order supermodes.⁹

The near-field intensity pattern of a buried-ridge phased array operating at $1.25 \times I_{th}$, measured parallel to the junction plane, is shown in Fig. 3. The small modulation in this field pattern is an indication of the large coupling between the channel fields, made possible by the soft index guiding of the channels and their close proximity. This small modulation also implies that mainly the fundamental supermode is excited. The asymmetry in the near-field pattern is believed to be a result of inadvertent differences in the channel parameters¹¹ (e.g., their widths or effective index steps). The smaller excitation of the outermost channels, compared with that of the inner ones, is a feature of the supermode near-field pattern. For the fundamental supermode in an eight-element, uniform array, the intensity in the outermost channels is only 12% of that in the central ones.⁹ This rela-

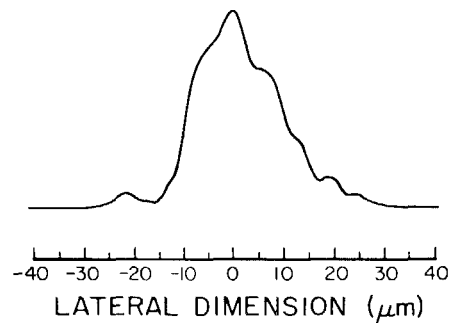


FIG. 3. Measured near-field pattern, in the junction plane, of a buried-ridge phased array. $I = 500$ mA ($I_{th} = 400$ mA).

tive intensity may be even smaller in nonuniform arrays.^{9,11}

The efficient phase locking among the elements of the buried-ridge phased arrays, as demonstrated by the far-field patterns in Fig. 2, is a result of the large optical coupling between the array channels and the uniform gain distribution across the array. The large coupling coefficient minimizes the effect of differences in the channel propagation constants on the supermode near-field and far-field patterns. Such differences, when large compared to the coupling coefficient, may reduce the number of array channels which are effectively excited in a given supermode, thus leading to a larger beam divergence than expected.¹¹ The actual gain distribution in the active layer, below the grooved section (see Fig. 1), depends on the relative resistivities of the p -InP and the p -InGaAsP ($\lambda_g = 1.2 \mu\text{m}$) layers, as well as on the depth of the grooves and the channel separation. For the device parameters described above, it is expected that the gain in the array channels is comparable to that in the region between them. Therefore, the modal gain of the fundamental supermode is higher than that of the highest order one whose near-field pattern is characterized by intensity nulls in the interchannel regions.⁹

Indeed, most of the buried-ridge arrays exhibited a nar-

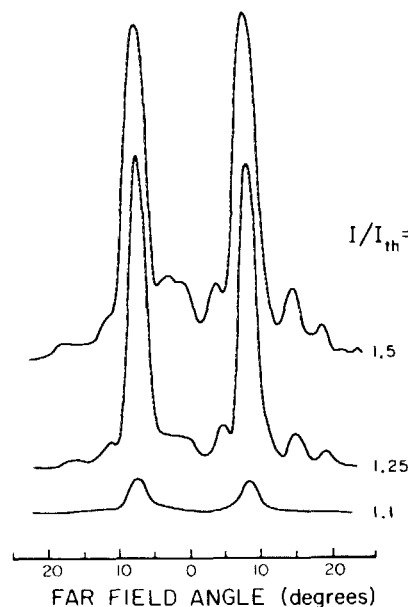


FIG. 4. Far-field pattern of a buried-ridge array operating mainly in the highest order supermode.

row single lobed beam, which indicates oscillation in the fundamental supermode. However, one of the arrays that were tested (out of about two dozen) showed a double lobed far-field pattern, which is shown in Fig. 4. The angular separation between the main lobes was 15° , which agrees well with the calculated separation for the highest order supermode ($\nu = 8$), 14.9° .⁹ The domination of the highest order supermode, in this case, may be the result of deeper grooves or inadvertent, larger doping difference between the p -InP and the p -InGaAsP layers, which led to more lossy interchannel regions.

In summary, we reported on the performance of phased arrays of buried-ridge InP/InGaAsP lasers, emitting at $1.3 \mu\text{m}$. These arrays are characterized by strong interchannel coupling and exhibit single lobed far fields, less than 4° wide, up to more than twice the threshold current. The field patterns of these arrays indicate that they oscillate mainly in the fundamental array supermode.

The research reported in this paper is supported through contracts with the National Science Foundation, the Office of Naval Research, and the Air Force Office of

Scientific Research. E. Kapon would like to acknowledge the support of a Weizmann Postdoctoral Fellowship.

¹D. R. Scifres, C. Lindstrom, R. D. Burnham, W. Streifer, and T. Paoli, *Electron. Lett.* **19**, 169 (1983) and references therein.

²D. E. Ackley and R. W. H. Engleman, *Appl. Phys. Lett.* **39**, 27 (1981).

³D. Botez and J. C. Connolly, *Appl. Phys. Lett.* **43**, 1096 (1983).

⁴J. Katz, E. Kapon, C. Lindsey, U. Shreter, S. Margalit, and A. Yariv, *Appl. Phys. Lett.* **43**, 521 (1983).

⁵W. T. Tsang, N. A. Olson, and R. A. Logan, *Appl. Phys. Lett.* **42**, 1003 (1983).

⁶E. Kapon, J. Katz, S. Margalit, and A. Yariv, *Appl. Phys. Lett.* **44**, 157 (1984).

⁷E. Kapon, Z. Rav-Noy, L. T. Lu, M. Yi, S. Margalit and A. Yariv, *Appl. Phys. Lett.* **45**, 1159 (1984).

⁸T. R. Chen, K. L. Yu, B. Chang, A. Hasson, S. Margalit, and A. Yariv, *Appl. Phys. Lett.* **43**, 136 (1983).

⁹E. Kapon, J. Katz, and A. Yariv, *Opt. Lett.* **9**, 125 (1984).

¹⁰It should be noted that even shallow grooves may result in large variations in the effective index. This happens when the p -InGaAsP layer supports a mode whose effective index is equal to that of the mode guided by the active layer. In that case, the etched grooves may not be regarded as a small perturbation, and, therefore, the supermodes should be found by employing a three-dimensional waveguide analysis.

¹¹E. Kapon, C. P. Lindsey, J. Katz, S. Margalit, and A. Yariv (unpublished).